

POLITECNICO DI TORINO
Repository ISTITUZIONALE

Single-frequency, pulsed Yb³⁺-doped multicomponent phosphate power fiber amplifier

Original

Single-frequency, pulsed Yb³⁺-doped multicomponent phosphate power fiber amplifier / Balliu, Enkeleda; Boetti, NADIA GIOVANNA; Pugliese, Diego; Lousteau, Joris; Engholm, M.; Milanese, Daniel; Nilsson, Hans-Erik. - In: JOURNAL OF OPTICS. - ISSN 2040-8978. - ELETTRONICO. - 22:11(2020), p. 115606. [10.1088/2040-8986/abbb5f]

Availability:

This version is available at: 11583/2848302 since: 2020-10-13T15:46:13Z

Publisher:

IOP Publication

Published

DOI:10.1088/2040-8986/abbb5f

Terms of use:

This article is made available under terms and conditions as specified in the corresponding bibliographic description in the repository

Publisher copyright

IOP postprint/Author's Accepted Manuscript

"This is the accepted manuscript version of an article accepted for publication in JOURNAL OF OPTICS. IOP Publishing Ltd is not responsible for any errors or omissions in this version of the manuscript or any version derived from it. The Version of Record is available online at <http://dx.doi.org/10.1088/2040-8986/abbb5f>

(Article begins on next page)

Single-frequency, pulsed Yb³⁺-doped multicomponent phosphate power fiber amplifier

ENKELEDA BALLIU¹, NADIA G. BOETTI², DIEGO PUGLIESE³, JORIS LOUSTEAU⁴, MAGNUS ENGHOLM¹, DANIEL MILANESE⁵, AND HANS-ERIK NILSSON⁶

¹ Mid Sweden University, Division of Electronics Design, 851 70 Sundsvall, Sweden

² LINKS Foundation - Leading Innovation and Knowledge for Society, Via P. C. Boggio 61, 10138 Torino, Italy

³ DISAT - Politecnico di Torino and RU INSTM, C.so Duca degli Abruzzi 24, 10129 Torino, Italy

⁴ CMIC - Politecnico di Milano, Via Mancinelli 7, 20131 Milano, Italy

⁵ DIA - Università di Parma and RU INSTM, Parco Area delle Scienze 181/A, 43124 Parma, Italy

⁶ Mid Sweden University, Faculty of Science, Technology and Media, 851 70 Sundsvall, Sweden

E-mail: enkeleda.balliu@miun.se

Received xxxxxx

Accepted for publication xxxxxx

Published xxxxxx

Abstract

High-power, single-frequency, pulsed fiber amplifiers are required in Light Detection And Ranging (LiDAR), coherent laser detection, and remote sensing applications to reach long range within a short acquisition time. However, the power-scaling of these amplifiers is limited by nonlinearities generated in the optical fibers, in particular by stimulated Brillouin scattering (SBS). In this regard, the use of multicomponent phosphate glasses maximizes the energy extraction and minimize nonlinearities. Here, we present the development of a single-stage, hybrid, pulsed fiber amplifier using a custom-made multicomponent Yb-doped phosphate fiber. The performance of the phosphate fiber was compared to a commercial Yb-doped silica fiber. While the latter showed SBS limitation at nearly 6.5 kW for 40 cm length, the maximum achieved output peak power for the multicomponent Yb-doped phosphate fiber was 11.7 kW for 9 ns pulses using only 20 cm with no sign of SBS.

Keywords: single-frequency, Yb-doped phosphate fiber, high-power, single-stage master-oscillator power fiber amplifier

1. Introduction

The continuous progress of drone technologies combined with coherent LiDAR systems keeps generating new applications and opening new opportunities [1]. For LiDAR and other related applications, such as remote sensing and coherent laser detection, the coherence, output peak power, and size of the laser source are of indeed paramount importance. Amongst the most successful laser

configurations, the hybrid master-oscillator power fiber amplifier (MOPFA) offers compactness and a high output peak power [2–4]. This optical fiber-based amplification configuration has been widely studied and refined over the last two decades. Typically, it consists of a diode-pumped solid-state or semi-conductor-based laser used as a master oscillator followed by one or more fiber amplifying stages. The implementation of a MOPFA relies foremost on commercial silica glass-based optical fiber technology which

has been key in the successful development of high power fiber lasers and amplifiers [5-7].

The high purity of the silica glass material produced through modified chemical vapor deposition (MCVD) combined to the outstanding intrinsic thermo-mechanical properties of silica glass have allowed to develop low loss optical fiber amplifiers able to handle several kW of optical power in the continuous wave (CW) regime [8-11]. Other benefits of the silica glass fiber technology includes flexibility, cost-effective high volume production and, more importantly, easy integration through “standard” splicing procedure.

However, the exploitation of this latter technology in the pulsed-regime appears less trivial. Actually, one key limitation of silica glass matrix is the limited concentration of Rare-Earth (RE) ions (~ 0.6 mol% Yb_2O_3) achievable while remaining free of clustering effect [12]. As the concentration increases above this value, in most of the cases the RE ions tend to cluster leading to nonradiative quenching of the electronic excited states. The quenching not only decreases the efficiency of the overall conversion of the absorbed pump source but also, as a consequence, generates heat in the system. The limited concentration of RE ions/unit length implies a limited optical gain/unit length and thus the requirement for long amplifying fiber lengths. This latter feature is not a particular issue when operating in CW regime but it becomes an impairing feature for propagating pulses with substantial peak power because of the onset of optical nonlinearities in the optical fiber, in particular the SBS. SBS arises from the interaction of acoustic phonons with the propagating signal wave, which is converted into a frequency-shifted, backward-propagating signal [13].

In silica glass optical fiber numerous suppression techniques have been implemented. Some techniques, such as temperature gradient [14] and strain gradient techniques [4, 15], involved the mitigation of the SBS applied directly onto the fiber. With the aim to mitigate the SBS, substantial research activities on the fiber configuration (geometry, morphology) have been also reported. These works include in particular studies on large-mode-area fibers [16, 17], nonuniform fibers [18], fibers with a transverse acoustic waveguide design [19], and highly doped fibers [20]. The use of highly doped fibers, in particular, has resulted to be extremely effective in the SBS suppression. Indeed, increasing the Yb^{3+} ions concentration/unit length increases the pump absorption and optical gain/unit length. The desired optical amplification can thus be achieved over a shorter fiber length implying a higher SBS threshold. However, a high Yb^{3+} ions concentration in the silica host can eventually lead to undesirable high-concentration drawbacks such as quenching [21], photodarkening [22], and mode instability when large core dimensions are concerned [23].

Therefore, in this work we have applied an alternative SBS suppression technique by using multicomponent phosphate fibers. Thanks to their high solubility of RE ions and weak ion-ion interactions [24, 25], multicomponent phosphate glasses can be doped with large amounts of RE ions (up to 10^{21} ions/cm³) without clustering [26, 27]. This

enables the realization of an active medium with a high optical gain in a short length and thus the mitigation of nonlinear optical effects [28]. Known to be excellent host materials for optical amplifiers and lasers, phosphate glasses possess excellent thermomechanical properties [29], high optical damage threshold and immunity to photodarkening [30]. The SBS gain coefficient in the phosphate fiber has been shown to be 50% lower than that of silica [31].

Despite these advantages, the use of phosphate-based fibers still suffers from limitations compared to the silica-based fibers. The major bottleneck is their low glass transition temperature (~ 500 °C), which makes challenging the splicing process between those two types of fibers and, hence, their integration as a single laser system. Several studies have successfully addressed some of these limitations in developing performant laser sources [32] using standard as well as polarization-maintaining (PM) phosphate fibers [33]. Despite the outstanding achievements mentioned above, there is substantial scope for improving these latter, thus making the development of phosphate glass-based fiber lasers a very active R&D field.

To date, several studies have been reported on high-power, single-frequency phosphate fiber amplifiers operating both in CW [34-36] and pulsed modes [33, 37-40] in the 1.5 μm wavelength range and very few demonstrate the amplification of pulse-light using Yb-doped phosphate fibers (see Table 1).

Table 1. Selected Works on Single-Frequency, Pulsed Yb-Doped Fiber Amplifiers

Ref.	Wavelength (nm)	Nr. of amp. stages	Active fiber core/cladding diam. (μm)	Fiber length (m)	Pulse duration (ns)	Rep. rate (kHz)	Peak power (kW)
Akbulut et al. [33]	1064.00	2	25/n.a.	0.25	100	10	1.20
Leigh et al. [37]	1550.67	3	15/122	0.12	~ 7	5	51.50
Shi et al. [38]	1530.00	3	25/400	0.15	105	8	1.20
This work	1064.00	1	20/176	0.20	9	19	12.00

The highest peak powers achieved for a single-frequency, pulsed, phosphate fiber amplifier were 51.5 kW from Leigh et al. [37] at 1550.67 nm and 3.15 kW developed by Fu et al. [40] at 1064 nm. However, these results were obtained using several amplification stages, and the phosphate fiber was used only in the last amplification stage. The use of more than one amplification stage increases the cost, size and complexity of the fiber amplifier and does not fully exploit the benefits of using phosphate-based fibers. Thus far, to the

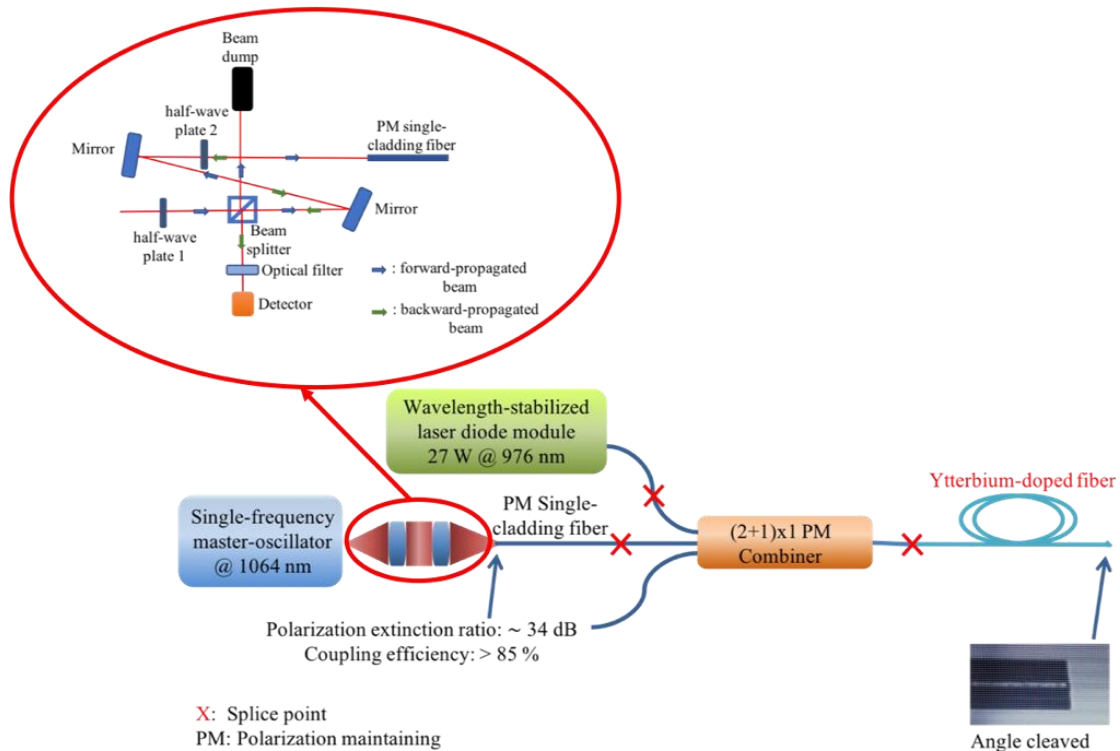


Figure 1. Simplified scheme of a pulsed, single-stage hybrid fiber amplifier operating at 1064 nm. The light emitted from a seed laser is coupled into a single-cladding fiber through a free-space coupling system. The single-cladding polarization maintaining (PM) fiber is spliced to the input signal fiber of a polarization-maintaining combiner. The fiber amplifier is pumped by a wavelength-stabilized pump diode operating at 976 nm. The output signal fiber of the PM combiner is spliced to the Yb-doped fiber, which is angle-cleaved at one end at an angle of 8° to avoid Fresnel's reflections. Inset: Setup used for the measurement of the SBS signal. The backward-propagated signal propagates in the same manner, but in a different direction, as the forward seed signal. As the signal is linearly polarized, depending on half-wave plate 2, the backward-propagated signal will travel toward the seed laser or detector. Before reaching the detector, the signal is filtered to remove any residual pump power, which is reflected from the fiber.

best of our knowledge, the use of Yb-doped multicomponent phosphate fibers for the power-scaling of a pulsed single-frequency and narrow-linewidth fiber amplifier at 1 μm in only one amplification stage has not been reported yet. In this work, we present preliminary results towards the development of a high peak power pulsed single-frequency laser through the use of a single amplification stage in a MOPFA configuration. The amplifying fiber consists in a novel, custom-made, single-cladding, Yb-doped multicomponent phosphate fiber. The maximum achieved output peak power was 11.7 kW using only 20 cm of the Yb-doped phosphate fiber.

2. Experimental setup

2.1 Single-frequency hybrid fiber amplifier design

The experimental setup of the fiber amplifier is illustrated in Figure 1. The fiber amplifier is a hybrid MOPFA consisting of a 1064-nm passive Q-switched laser used as a seed laser (see Section 2.2), followed by an amplification stage. Light from the master oscillator was free-space-coupled with a coupling efficiency of more than 85% into a single-cladding PM fiber with core/cladding dimensions of

20/125 μm (see inset of Figure 1). The single-cladding PM fiber was spliced to the input signal fiber of a pump/signal (2+1)x1 PM combiner (ITF Technologies, Canada). The combiner is composed of two standard pump fibers (105/125 μm) and one PM signal fiber (20/125 μm) with a core numerical aperture (NA) of 0.08. The Yb-doped fibers were forward-pumped into the cladding by one wavelength-stabilized fiber-coupled pump diode module (BWT Beijing, China), which operates at 976 nm and delivers a maximum pump power of 27 W. The fiber-coupled pump diode modules were spliced to the 105/125 μm pump fiber of the PM combiner. The SBS signal was measured from the backward-propagated signal through a beamsplitter cube positioned after the laser (see inset of Figure 1) and the SBS onset is defined as the point where the backward-propagating power starts to increase nonlinearly with pump power. The output signal fiber of the PM combiner was spliced to the Yb-doped fibers, namely the 20/125 μm silica host-based and the in-house developed 20/176 μm phosphate fiber (see Section 2.3). The Yb-doped phosphate fiber was manufactured as a single-cladding fiber without any coating; therefore, it was recoated along the length (see Section 2.3.1). The active fibers were cleaved at one end at an angle of 8° to avoid Fresnel's reflections. The set-up used for the measurement of SBS signal is shown in the inset of Figure 1.

2.2 Master Oscillator

The 1064 nm, passive Q-switched, single-frequency master oscillator was manufactured by Cobolt (Hübner Group Company, Germany). The high-finesse laser cavity is an unidirectional ring cavity with three cavity mirrors, which constitute a triangle with two sides of equal length. The intra-cavity field at 1064 nm rotates anticlockwise around the cavity perimeter; the cavity length is approximately 50 mm and is pumped through the curved mirror by two laser diodes at 808 nm with a maximum attainable output power level up to 4 W. The laser crystal is Nd:YAG with a dopant level of 1% and a length of 3 mm. An optical isolator was inserted in the cavity to force the laser to run unidirectionally. A Cr:YAG crystal was inserted, acting as a passive Q-switch. This laser generates an average polarized output power of up to 1 W with a polarization extinction ratio (PER) higher than 30 dB. The Gaussian pulses exhibit a pulse width and repetition rate of 9 ns and 19.1 kHz, respectively. Because of its narrow linewidth, this seed laser is very sensitive to SBS. The average power level where the SBS occurs at the output of the combiner, without any active fiber, is 0.5 W. Therefore, in our experiments, we only used 0.4 W of the average output power from the seed laser.

2.3 Characteristics of the Yb³⁺-doped fibers

The characteristics of the active fibers used in this work are summarized in Table 2. The commercially available silica fiber and the in-house developed phosphate fiber exhibit a core absorption of 1185 dB/m at 976 nm and of 3730 dB/m at 975 nm, respectively. The core absorption spectra in dB/m for both fibers are shown in Figure 2.

Fiber under test	Core absorption (dB/m)	Core numerical aperture	Core/cladding diameters (μm)
Yb-doped silica fiber	1185 at 976 nm	0.08	20/125
Yb-doped phosphate fiber	3730 at 975 nm	0.06	20/176

Table 2. Characteristics of the Yb-doped fibers

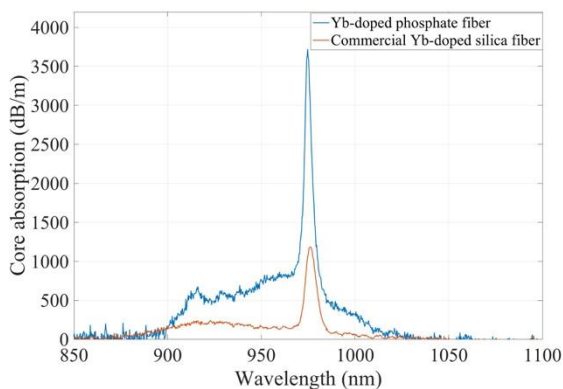


Figure 2. Core absorption spectra of Yb-doped phosphate- and silica-based glass fibers.

2.3.1 Material properties of the Yb³⁺-doped phosphate fiber

The active phosphate fiber was manufactured by preform drawing, with the preform being obtained by the rod-in-tube technique. The drawing tower furnace (SAET, Turin, Italy) consists of a graphite ring heated by induction operating at 248 kHz and delivering 170 W to reach the required drawing temperature. High-purity (99+%) chemicals (P₂O₅, K₂O, Al₂O₃, B₂O₃, SiO₂, PbO, La₂O₃) were weighed and mixed inside a glove box under dried air atmosphere to minimize the hydroxyl ions (OH⁻) content in the glass. Afterward, they were transferred in a Pt crucible for melting in a vertical furnace at a temperature of 1400 °C for 1 h under a controlled atmosphere (dry air, water content < 3 ppm). The core glass was doped with 2.4 mol% of Yb₂O₃, corresponding to a concentration of the Yb³⁺ ions of 6.15×10^{20} ions/cm³. Then, it was cast into a cylindrical mold to form a rod, whereas the cladding glass tubes were shaped by rotational casting (at a rotation speed of 3000 rpm) using an in-house-developed equipment. The cast glasses were immediately annealed at a temperature around the transition temperature, T_g , for 5 h to relieve internal stresses and finally cooled down slowly to room temperature. The fluorescence lifetime of the $^2F_{5/2} \rightarrow ^2F_{7/2}$ transition of Yb³⁺ ions in the core glass was measured to be 1.0 ± 0.1 ms. The lifetime value agrees with the scientific literature, thus demonstrating no quenching of the RE ions. The calculated absorption cross-section was 1.27×10^{-24} cm² at 974.6 nm. The refractive index of the core and cladding glasses was measured with a prism coupler (Metricon Model 2010) at 1061 nm and revealed to be 1.5439 ± 0.0005 and 1.5428 ± 0.0005 , respectively.

Scanning electron microscopy cross-sectional images of the fabricated single-cladding phosphate glass fiber showed core/cladding diameters of 20/176 μm with a core NA of 0.06 at 1.06 μm (see Figure 3a). A 20 μm core diameter implies the fiber being few-mode at 1064 nm despite the low NA value. The purpose of a large core was both to assess integration feasibility and to demonstrate amplification ability. Although it requires subtle glass process control and adjustments of the glass fabrication process, a low NA value is achievable to satisfy single-mode (SM) operation in a 20 μm core. For this first demonstration, where SM operation is not critical, we opted for a conservative approach targeting a NA value of 0.06. The large outer diameter of 176 μm, as compared to the standard 125 μm diameter of commercial silica glass fibers, provides further mechanical strength to the uncoated phosphate fiber. The quality and morphology of the fabricated phosphate glass optical fiber were inspected by means of a Nikon ECLIPSE E 50i optical microscope. Fiber losses were measured by the cut-back technique using a

length of about 250 cm with a SM fiber pigtailed laser diode source operating at 1300 nm.

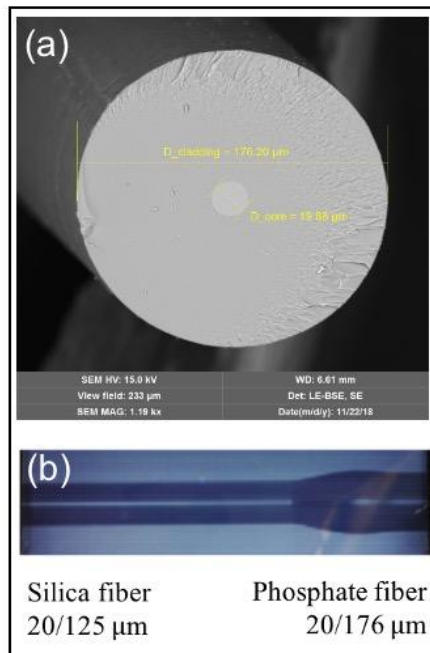


Figure 3. (a) Scanning electron microscopy cross-sectional image of the single-cladding Yb-doped phosphate fiber. (b) Image of the splicing of the silica passive fiber (20/125 μm) with the Yb-doped phosphate fiber (20/176 μm).

The attenuation value was calculated through linear least-squares fitting of the experimental data and was equal to 1.1 dB/m. In order to assess the guiding properties of the fiber, a set of near-field images of the fiber cross-section was measured on a 250 cm-long fiber piece, at the wavelength of 1300 nm, using a butt-coupled fiber pigtailed laser diode source. The light beam was found to be well-confined inside the core, and only a negligible diffused area was observed inside the cladding. As the fiber is single-cladding, a recoating process (see Section 2.3.2) was crucial to reduce its long-term sensitivity to external environmental factors. The active fiber was cooled simply by conduction by placing it on a V-groove metallic plate (HFV002, Thorlabs).

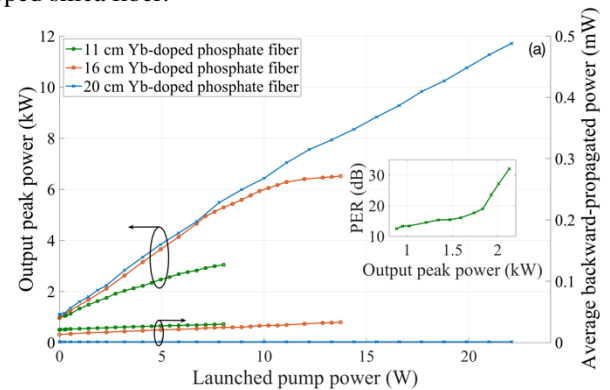
2.3.2 Splicing and coating of the Yb^{3+} -doped phosphate fiber

The active phosphate fiber was first cleaved on both ends and then recoated. The recoating was carried out using a Vytran PTR-200-MRC recoater and an acrylate UV-sensitive solution from Efirion (UVF PC-373), which shows a refractive index of 1.373 at the wavelength of 852 nm. The maximum coating length possible with this coating was 50 mm; hence, several recoating processes were required to cover the whole length of the active fiber. The fiber was left without coating at both ends: over a length of 20 mm at one

end of the fiber that was spliced to the silica fiber of the combiner and over a length of 3 mm at the other end that was cleaved at an angle of 8° . The splicing process was performed using an Ericsson FSU 995 PM splicer. The lower glass transition temperature of the phosphate fiber ($\sim 500^\circ\text{C}$) compared to that of the silica fiber ($\sim 1000^\circ\text{C}$) made the silica-phosphate fiber splicing process challenging, as well as the thermal management of the splicing point complicated. Therefore, a special splicing program was developed to splice the single-cladding 20/176 μm Yb-doped phosphate fiber to the double-cladding 20/125 μm output signal fiber of the PM combiner (see Figure 3b). Nevertheless, the splice losses were typically less than 1 dB with yet substantial scope for further improvement through optimization of the process. An optimized splicing process and a good cooling method of the splicing point are important to avoid the danger of silica-to-phosphate fiber splice breakout during high-power operation due to the difference in thermal expansion coefficients of the two fibers.

3. Experimental results and discussion

The dependence of the SBS threshold on the fiber length requires the use of short active fibers [13]. Therefore, the active fiber lengths that were tested in the amplifier in this work were chosen based on the tradeoff between the onset of SBS and sufficient pump absorption, which is directly related to the slope efficiency. The performance of the fiber amplifier was first evaluated using different fiber lengths, namely 10, 16, and 20 cm of the custom-made, single-cladding 20/176 μm Yb-doped phosphate fiber, and then compared to different fiber lengths of a commercial Yb-doped silica fiber.



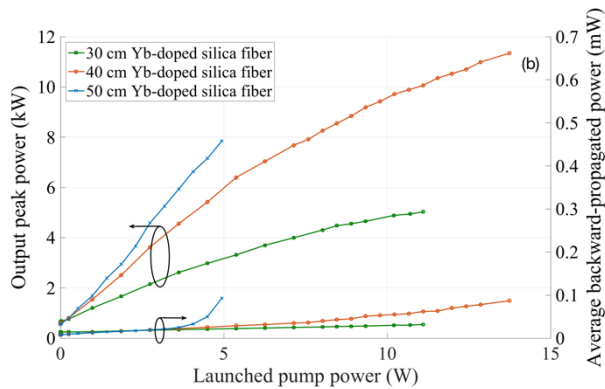


Figure 4. Output power of the fiber amplifier using different fiber lengths: (a) of the custom-made, single-cladding, 20/176 μm Yb-doped phosphate fiber and (b) of a commercial Yb-doped silica fiber. Inset: polarization extinction ratio of the 11 cm-long phosphate fiber at different launched pump powers.

In Figure 4a and 4b are shown the output peak power (left y-axis) and average backward-propagated power (right y-axis) of the custom-made phosphate fiber and of the commercial fiber respectively with respect to the launched pump power. Using 11 cm of phosphate fiber, we achieved a maximum output peak power of 2.8 kW before damaging the splicing point, most likely because of a high heat load in the active fiber and at this point in particular. A low slope efficiency of 23% demonstrates that the length of the active fiber was too short. The temperature of the fiber surface exceeded 60 °C, measured with a forward-looking infrared (FLIR) camera. The relatively high temperature along the optical fiber may be ascribed to the high pump power absorbed by the active gain medium in a short fiber length and to the scattering and absorption of pump power due to imperfections or inclusions in the phosphate glass or at the core/cladding interface.

For a slightly longer fiber (16 cm), the maximum output peak power and slope efficiency increased to 6.5 kW and 46%, respectively. Even though the slope efficiency increased, the observed gain saturation indicates that the length of the fiber was not optimal. Using 20 cm of the Yb-doped phosphate fiber, a maximum output peak power of 11.7 kW was achieved corresponding to an average power of nearly 2.4 W. The slope efficiency was identical to that of the 16 cm-long fiber, and no gain saturation was observed, indicating that the active fiber length of 20 cm was close to optimal considering all factors. However, further power scaling for this length was limited by the available pump power. No SBS was observed indicating that an even longer fiber could be used. The best performance of the fiber amplifier, achieved with the 20 cm-long Yb-doped phosphate fiber, was compared to the performance of different length of a commercial Yb-doped silica fiber. Despite the high pump absorption of the silica fiber, a fiber length of 30 cm revealed to be short, which results in a gain saturation even at a low launched pump power. To achieve similar output peak powers as the one measured in the case of the 20 cm-long Yb-doped phosphate fiber used in our experiment, a

commercial Yb-doped silica fiber almost double in length is necessary. However, for length higher than 30 cm, SBS will become a limit for further power scaling (see Figure 4b). The higher slope efficiency observed in this case with respect to the one of the Yb-doped phosphate fiber can be partly ascribed to the lower core/cladding area ratio. The inset of Figure 4a shows the polarization extinction ratio (PER) measurements for the 11 cm-long Yb-doped phosphate fiber. The polarization out of the seed laser was higher than 30 dB and, as the active fiber used was very short, the polarization was still maintained. The PER increased significantly with the increase in pump power, achieving a value higher than 25 dB at output peak powers higher than 1.8 kW. Further investigation is needed to explain this behavior; however, this increase in the PER may be ascribed to the stress induced into the fiber from the heat load when the temperature of the fiber increased. Another cause may be the presence of imperfections or inclusions in the phosphate glass, which can induce a one-directional stress into the fiber and therefore lead to an increase of the PER while enhancing the pump power. A slightly lower PER is expected in the case of longer fiber sections, and this is due to the fiber shape, which can be improved with future designs of an asymmetrical shape for the active phosphate fiber.

The optical spectrum in the forward direction was measured for all the Yb-doped phosphate fiber lengths. Figure 5 shows the optical spectrum for the case of the 20 cm-long fiber at the output peak power of 12 kW. The optical signal-to-noise ratio was 57 dB, and no distortion of the pulses could be observed after amplification (see inset of Figure 5).

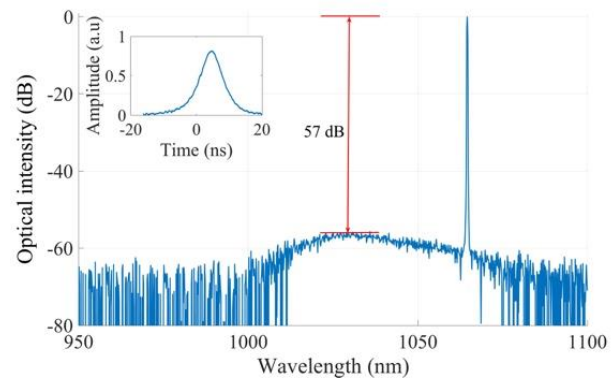


Figure 5. Normalized signal-to-noise ratio of the output signal of the fiber amplifier using 20 cm of the active phosphate fiber. Inset: measured beam pulse shape.

4. Conclusion

We demonstrated important foundation results towards the development of a pulsed single-amplification-stage, single-frequency fiber amplifier using the relatively short fiber length of a novel, custom-made 20/176 μm Yb-doped

phosphate fiber, achieving output peak powers of up to 12 kW without any sign of SBS. This was accomplished using only 20 cm of this novel fiber. Further power scaling was limited by the high thermal load, and an additional increase in the output peak power scaling will require future ongoing improvements of the Yb-doped phosphate fiber. A decrease of the phosphate glass fiber outer diameter towards the more standard 125 μm value will reduce residual stress and improve thermal loading at the splice interface with the pump/signal delivery silica glass fiber. We anticipate that SM operation will also contribute improving the amplification efficiency and reduce injection losses at the splice interface.

The implementation of a double-cladding structure and, in particular, an all-glass double-cladding structure, i.e. without using any polymer for the second cladding, would also be beneficial for exploiting efficiently the pump power through the fiber. Phosphate glasses allow a much higher compositional flexibility compared to silica, which enables the realization of a high NA for the first cladding (up to 0.46), thus avoiding the use of polymers, which intrinsically display a much poorer thermal stability than glasses. Furthermore, an improvement in the splicing process and its cooling will lead to a higher output peak power without adding additional amplification stages. Our preliminary results confirm the possibility of realizing ultra-compact single-stage power fiber amplifiers. Key fiber features will be optimized through ongoing work. Besides onboard applications, the new laser source could also prove useful for the generation of high-output-peak-power laser sources operating at 532 and 355 nm via frequency doubling and tripling.

Funding

EU Regional funds (135790); Knowledge Foundation (KKS); Region Västernorrland (0868895); Interdepartmental Center PhotoNext of Politecnico di Torino.

Acknowledgements

Cobolt, a Hübner Group Company, Nyfors Teknologi AB and ITF Technologies (Canada) are gratefully acknowledged for their support.

References

- [1] Kellner J R, Armston J, Birrer M, Cushman K C, Duncanson L, Eck C, Fallegger C, Imbach B, Král K, Krůček M, Trochta J, Vrška T and Zraggen C 2019 *Surv. Geophys.* **40** 959
- [2] Limpert J, Höfer S, Liem A, Zellmer H, Tünnermann A, Knoke S and Voelckel H 2002 *Appl. Phys. B* **75** 477
- [3] Di Teodoro F, Koplow J P, Moore S W and Kliner D A V 2002 *Opt. Lett.* **27** 518
- [4] Balliu E, Engholm M, Hellström J, Elgerona G and Karlsson H 2014 *Proc. SPIE* **8959** 895910
- [5] Zervas M N and Codemard C A 2014 *IEEE J. Sel. Top. Quantum Electron.* **20** 0904123
- [6] Canat G, Augère B, Besson C, Dolfi-Bouteyre A, Durécu A, Goular D, Le Gouët J, Lombard L, Planchat C and Valla M 2016 *Conference on Lasers and Electro-Optics (CLEO)*, San Jose, 2016, pp. 1-2
- [7] Liu C, Qi Y, Ding Y, Zhou J, Dong J, Wei Y and Lou Q 2011 *Chin. Opt. Lett.* **9** 031402
- [8] Platonov N, Yagodkin R, De La Cruz J, Yusim A and Gapontsev V 2018 *Proc. SPIE* **10512** 105120E
- [9] Lin H, Tao R, Li C, Wang B, Guo C, Shu Q, Zhao P, Xu L, Wang J, Jing F and Chu Q 2019 *Opt. Express* **27** 9716
- [10] Qi Y, Yang Y, Shen H, He B and Zhou J 2017 *Laser Congress (ASSL, LAC)*, Nagoya, 2017, pp. 1-3.
- [11] Beier F, Hupel C, Kuhn S, Hein S, Nold J, Proske F, Sattler B, Liem A, Jauregui C, Limpert J, Haarlammer N, Schreiber T, Eberhardt R and Tünnermann A 2017 *Opt. Express* **25** 14892
- [12] Unger S, Schwuchow A, Dellith J and Kirchhof J 2020 *Opt. Mater. Express* **10** 907
- [13] Agrawal G 2012 *Nonlinear Fiber Optics*, 5th ed. (Amsterdam: Elsevier Science Publishing Co.).
- [14] Kovalev V I and Harrison R G 2006 *Opt. Lett.* **31** 161
- [15] Zhang L, Cui S, Liu C, Zhou J and Feng Y 2013 *Opt. Express* **21** 5456
- [16] Limpert J, Liem A, Reich M, Schreiber T, Nolte S, Zellmer H, Tünnermann A, Broeng J, Petersson A and Jakobsen C 2004 *Opt. Express* **12** 1313
- [17] Robin C, Dajani I and Pulford B 2014 *Opt. Lett.* **39** 666
- [18] Liu A 2007 *Opt. Express* **15** 977
- [19] Dong L 2010 *J. Lightwave Technol.* **28** 3156
- [20] Balliu E, Engholm M and Nilsson H -E 2019 *Proc. SPIE* **10896** 1089618
- [21] Paschotta R, Nilsson J, Barber P R, Caplen J E, Tropper A C and Hanna D C 1997 *Opt. Commun.* **136** 375
- [22] Koponen J J, Söderlund M J, Hoffman H J and Tammela S K T 2006 *Opt. Express* **14** 11539
- [23] Tao R, Ma P, Wang X, Zhou P and Liu Z 2016 *Laser Phys.* **26** 065103
- [24] Delevaque E, Georges T, Monerie M, Lamouler P and Bayon J -F 1993 *IEEE Photonics Technol. Lett.* **5** 73
- [25] Gapontsev V P, Matitsin S M, Isineev A A and Kravchenko V B 1982 *Opt. Laser. Technol.* **14** 189
- [26] Lee Y -W, Sinha S, Digonnet M J F, Byer R L and Jiang S 2008 *Proc. SPIE* **6873** 68731D
- [27] Pugliese D, Boetti N G, Ceci-Ginistrelli E, Gallichi-Nottiani D, Janner D, Lousteau J and Milanese D 2018 *20th International Conference on Transparent Optical Networks (ICTON)*, Bucharest, 2018, pp. 1-4
- [28] Boetti N G, Pugliese D, Ceci-Ginistrelli E, Lousteau J, Janner D and Milanese D 2017 *Appl. Sci.* **7** 1295
- [29] Martin W and Milam D 1982 *IEEE J. Quantum Electron.* **18** 1155
- [30] Lee Y -W, Sinha S, Digonnet M J F, Byer R L and Jiang S 2008 *Electron. Lett.* **44** 14
- [31] Lee Y -W, Urbanek K E, Digonnet M J F, Byer R L and Jiang S 2007 *Proc. SPIE* **6469** 64690L
- [32] <http://www.npphotonics.com>

- [33] Akbulut M, Miller A, Wiersma K, Zong J, Rhonehouse D, Nguyen D and Chavez-Pirson A 2014 *Proc. SPIE* **8961** 89611X
- [34] Lee Y -W, Digonnet M J F, Sinha S, Urbanek K E, Byer R L and Jiang S 2009 *IEEE J. Sel. Top. Quantum Electron.* **15** 93
- [35] Bai X, Sheng Q, Shi W, Zhang H and Yao J 2016 *Proc. SPIE* **9728** 972835
- [36] Wu J, Zhu X, Temyanko V, LaComb L, Kotov L, Kiersma K, Zong J, Li M, Chavez-Pirson A, Norwood R A and Peyghambarian N 2017 *Opt. Mater. Express* **7** 1310
- [37] Leigh M, Shi W, Zong J, Yao Z, Jiang S and Peyghambarian N 2008 *Appl. Phys. Lett.* **92** 181108
- [38] Shi W, Petersen E B, Leigh M, Zong J, Yao Z, Chavez-Pirson A and Peyghambarian N 2009 *Opt. Express* **17** 8237
- [39] Shi W, Petersen E B, Yao Z, Nguyen D T, Zong J, Stephen M A, Chavez-Pirson A and Peyghambarian N 2010 *Opt. Lett.* **35** 2418
- [40] Fu S, Shi W, Tang Z, Shi C, Bai X, Sheng Q, Chavez-Pirson A, Peyghambarian N and Yao J 2018 *Proc. SPIE* **10512** 1051219